On the energy transport in a non-integrable Ising chain

João S. Ferreira[1]

[1] *CeFEMA, Instituto Superior Técnico, Universidade de Lisboa Av. Rovisco Pais, 1049-001 Lisboa, Portugal*

We study the energy transport, at finite and infinite temperatures, of a non-integrable spin chain employing typicality arguments. We characterize the relaxation dynamics after a local quench which drives the system away from equilibrium. At intermediate times, we observe that transport at infinite temperatures is diffusive. However, within the chain sizes available to our numerical methods, we observe a ballistic component in the energy propagation with an amplitude two orders of magnitude smaller than the diffusive one, yet to be characterized. At finite temperature, for short times, below a time scale τ, we find numeric evidence of ballistic transport. For times larger than τ the diffusion component dominates the transport. With decreasing temperatures both τ and the diffusive coefficient increase exponentially, while the velocity characterizing the ballistic component seems to remain constant. The dependence of the transport on the magnitude of the local quench was also studied at infinite temperature. We report a polynomial dependence of the diffusion constant with the magnitude of the quench.

Finally, we show that the time dependent variational principle for MPS algorithm fails to provide an improvement when compared with Lanczos-based methods for the available bound dimensions and system sizes.

I. Introduction

Transport in (quasi) one dimensional strongly correlated systems poses formidable theoretical and experimental challenges. On the theoretical side, the limited set of available tools, designed to study ground state and equilibrium properties, often provide an inadequate or inefficient description regarding transport[1]. On the experimental side, the advent of ultra-cold gases[2,3] and ion traps[4] have allowed precise realizations of toy models[5,6] as benchmark for many theoretical predictions and provides fertile ground for new discoveries.

Recently, much work has been devoted to whether and how isolated correlated systems thermalize in an out-of-equilibrium situation. It is now established that integrable systems do not thermalize to the Gibbs ensemble, but rather to the generalized Gibbs ensemble[3,7]. The physical reason relates to the infinite number of conservation laws, which impose strong constrains on the dynamics of these systems. Examples of discrete integrable models include the famous lattice models like the spin-1/2 XXZ chain or the Fermi-Hubbard model[8]. This contrasts with non-integrable Hamiltonians which are expected to satisfy the Eigenstate Thermalization Hypothesis[9] and thermalize towards the canonical Gibbs ensemble. Notorious exceptions include many-body localized phases[10], Griffiths regions[11], among others[12], which we refer as localized systems.

Much less is known regarding how many-body systems evolve towards the respective equilibrium states. In the case of integrable systems, with gapless excitations, the existence of nontrivial local conservation laws leads to strictly ballistic/dissipationless transport at all temperatures. This corresponds to a non-vanishing Drude weight within the framework of linear response theory. The Drude peak is defined as the zero frequency singularity in the real part of the conductivity of the transported quantity. On the other hand, a vanishing Drude peak signals diffusive/dissipative transport. The relation between the Drude weight and integrability of systems is achieved via the Mazur's inequality[13]. Mazur established that a lower bound for the Drude weight can be obtained from the overlap of the current operator in question with all the conserved quantities of the model. In general, some current in an integrable system, e.g. energy or spin current, may have both a diffusive and a ballistic component[14]. Considerations in integrable models are possible with the help of Bethe ansatz methods[15,16], which cannot be extended to non-integrable Hamiltonians. The current understanding of non-integrable models is that they are asymptotically diffusive in time due to the absence of non-trivial local conservation laws, which strongly limit the dissipationless transport. Important exceptions include many-body localized systems where transport is sub-diffusive.

A useful connection can be drawn between transport quantities and local quench dynamics. The latter refers to a multitude of quench protocols that induce locally finite currents in spin or energy density after some parameter in the Hamiltonian is non-adiabatically changed. The time dependence of the spreading of these density perturbations dictates the nature of the transport. We can measure the spreading by means of the spacial variance σ^2 of the density or similar quantities. Diffusive dynamics corresponds to a square root spreading, $\sigma \propto \sqrt{Dt}$ with time, while ballistic transport implies $\sigma \propto v_B t$. D and v_B are, respectively, the diffusion constant and the butterfly velocity.

To simulate quench dynamics in non-integrable systems, the prevailing numerical methods include Exact Diagonalization (ED) and variants of time dependent DMRG (tDMRG). ED is severely constrained to very small system sizes[7,17,18], specially in low symmetry Hamiltonians (often the case in non-integrable models). On the other hand, the time scales probed by tDMRG

variants[19–21] fall short due to the build up of correlations during time evolution, but allow for the study of very large system sizes $L \approx 200$.

The goal of this paper is to study the relaxation dynamics, at finite and infinite temperatures, of a non-integrable spin chain after a localized quench in energy density drives the system out-of-equilibrium. We obtain traditional transport coefficients, diffusion constant D or butterfly velocity v_B, from the spreading of the local energy density and study the dependence on different quenches and temperatures. To simulate the time evolution of the quenched system, up to any desirable precision, we employ the concept of typicality[20,22–24]. In a sentence, we say that a given set of random states generated according to some measure is typical, if the average quantum expectation value of some observable $A(t)$ over the initial states is, with large probability, the expectation value computed using the canonical ensemble. Therefore, to understand the evolution of a given initial ensemble, it is enough to study how a few individual states relax towards equilibrium after a quench. This provides significant computational advantages when comparing to ED, since time evolution can be achieved via Lanczos scheme[20].

Long time relaxation dynamics of large systems are hard problems, that nevertheless, for some cases, can be overcome with Matrix Product States (MPS). Recent works[25–27] have successfully used MPS to extract equilibrium properties and capture long-time transport coefficients at infinite temperature in large lattices. In this work, we attempt to use an initial ensemble of random MPS to simulate the dynamics of large spin chains and evolve it according to the Time Dependent Variational Principle for MPS algorithm (TDVP-MPS)[27,28]. The advantages of this scheme, in comparison to more standard tDMRG approaches, is that it preserves conservation laws throughout the evolution.

The structure of the paper is as follows: in Sec. II we introduce the spin-1/2 transverse/longitudinal field Ising model which we will use for time-evolving and also explain our quenching protocol as well as the quantity used to measure the spreading of energy. Sec. III is devoted to the study of transport at infinite temperatures for different system sizes and quench parameters. In Sec. IV we focus on the temperature dependence and the emergence of ballistic transport for intermediate times. Finally, Sec. V closes with a discussion of the results and possible directions of future works.

II. Model and method

As an example of non-integrable and non-localized models, we consider the spin-1/2 Ising chain with a transverse and longitudinal field (TLI) and open boundary conditions:

$$H_{\mathrm{TLI}} = J\sum_{i=1}^{L-1} S_i^x S_{i+1}^x + h\sum_{i=1}^{L} S_i^x + g\sum_{i=1}^{L} S_i^z \qquad (1)$$

with $S_i^{x,z}$ the spin matrices at site i and L an odd number of lattice sites. The Hamiltonian of Eq. (1) has only one known (discrete) symmetry, namely the reflection around the site $\lfloor L/2 \rfloor$. After probing the parameters space, we found that the non-integrability signatures of the system depend on the chosen parameters in such manner that integrable characteristics can emerge for short times. We wish to avoid these parameters choice which limit the study of long-time regimes in small system sizes. In particular, a careful choice of J, h and g should not only avoid the integrable lines at $J, g, h = 0$, but also avoid disparities in the relative magnitude of the parameters[29]. For the rest of this paper, we chose $J = 1.0$ $h = 1.15$ $g = 0.88$, which, as we will see, shows characteristic non-integrable transport.

To drive the system out-of-equilibrium, we apply the operator $Q(\epsilon) = \mathbb{I}(1-\epsilon) + \epsilon S^+_{\lfloor L/2 \rfloor}$ which acts on the middle of the chain at $t = 0$. The magnitude of the quench is quantified by the positive parameter ϵ. Strong quenches are defined as $\epsilon = 1$ whereas weak quenches have $\epsilon \gtrsim 0$. We can simulate the density matrix for $t > 0$,

$$\rho(t) = \frac{e^{-iHt}Q(\epsilon)e^{-\beta H}Q^\dagger(\epsilon)e^{iHt}}{\mathrm{Tr}\left(Q(\epsilon)e^{-\beta H}Q^\dagger(\epsilon)\right)} \qquad (2)$$

by means of the following asymptotically unbiased estimator r_β:

$$r_\beta = \frac{\sum_j^{N_s} e^{-iHt}Q(\epsilon)e^{-\beta H/2}\left|\psi_j\right\rangle\left\langle\psi_j\right|e^{-\beta H/2}Q^\dagger(\epsilon)e^{iHt}}{\sum_{j'}^{N_s}\left\langle\psi_{j'}\right|e^{-\beta H/2}Q^\dagger(\epsilon)Q(\epsilon)e^{-\beta H/2}\left|\psi_{j'}\right\rangle} \qquad (3)$$

where $\beta = 1/T$ is the inverse of temperature, N_s is the number of random states we sample from and $\{|\psi_i\rangle\}_{i=1}^{N_s}$ a set of normalized initial random states. Therefore, the thermal expectation value of any observable $A(t)$ can be computed as $\mathrm{Tr}\left(A(0)r_\beta\right)$. Note that the average over initial states should be taken independently on the denominator and the numerator in Eq. (3), otherwise the final expectation value is biased as shown in Ref.[30]. From a statistic perspective, $\mathrm{Tr}\left(A(0)r_\beta\right)$ is the expectation value of a statistical random variable which also has an associated standard error. We refer to the error of the observable as the region delimited by the standard error of the mean.

For small system sizes $L \leq 21$, we initialize the ensemble with the set of normalized random pure states (rPS) as introduced in Ref.[31]:

$$|\psi\rangle_{\mathrm{rPS}} = \frac{\sum_j^{2^L} c_j\left|j\right\rangle}{\left(\sum_j^{2^L}|c_j|^2\right)^{1/2}} \qquad (4)$$

where $\{|j\rangle\}_{j=1}^{d_H}$ is the computational basis of the Hilbert space and c_j a complex number parameterized by a real and imaginary part ($c_i = \eta_i + \mathrm{i}\xi_i$), each drawn from normal distributions of mean zero and variance one. Unfortunately, the required computational resources to simulate dynamics of quantum states grow exponentially

with the chain sizes. For chains larger than $L = 21$, we employ random MPS to initialize the ensemble. MPS are a special class of quantum states that can be written in the form:

$$|\psi\rangle_{\mathrm{MPS}} = \sum_{k_1 \ldots k_N} A^{(1)k_1} A^{(2)k_2} \ldots A^{(N)k_N} |k_1 k_2 \ldots k_N\rangle \quad (5)$$

where $\{|k_n\rangle\}_{j=1}^{d}$ is a basis of local states at site n, $A^{(n)\alpha_n}_{i_n,j_n}$ is a rank-3 tensor at position n with one physical index α_n and two non physical (bound) indices i_n, j_n respectively with dimensions d, χ_n and χ_{n+1} (where $\chi_n = min(\chi, d^n, d^{N-n})$). The parameter χ is the bound dimension of the MPS. The set of open boundary condition MPS, as defined above, can be shown to describe all states in the Hilbert space given a large enough bound dimension $\chi > 2^{L/2}$. However, the relevance of MPS is that for physically relevant states, the bound dimension necessary to describe the state can be kept small, $\chi \ll 2^{L/2}$, even in the thermodynamic limit. A key aspect of MPS is that, by construction, the entanglement entropy of a block of N sites, $S_E(N)$, is upperbounded for a given bound dimension and does not increase with the block's size, i.e. $\max S_E^{\chi} \propto \log \chi$. As long as the MPS description of some state ψ for a bound dimension χ satisfies $S_E^{\psi} < \max S_E^{\chi}$, the state is accurately described by the MPS description.

The time evolution of some initial state can also be performed in the manifold of MPS. However, in general, the entanglement entropy of a time evolved state is expected to grow in time leading to an inevitable saturation of S_E and a break down of the MPS description. This poses important time restriction to simulations using MPS. To delay the growth of entanglement entropy we initialize Eq. (3) using the set of random product states: $|\psi\rangle = \prod_l^L |i_l\rangle$ where each spin points randomly in the Bloch sphere,

$$|i_l\rangle = \cos\left(\frac{\theta_l}{2}\right)|\uparrow_l\rangle + e^{2i\phi_l} \sin\left(\frac{\theta_l}{2}\right)|\downarrow_l\rangle \quad (6)$$

and $\theta_l, \phi_l \in [0, \pi]$ are real random variables. Random product states have $S_E = 0$ and admit an exact MPS description with a bound dimension $\chi = 1$. To represent random product states with a larger bound dimension, it is enough to pad the remaining entries of the $A^{(n)}$ tensors with 0's[27]. We dthe MPS enoted MPS generated this way as product MPS (pMPS).

To evolve pMPS in real and imaginary time, we employ a time dependent variational principle for MPS (TDVP-MPS) scheme as introduced in Ref.[28]. Traditional methods solve the entanglement growth by projecting, at each time-step, the time evolved state back to the manifold of fixed bound dimension $\mathcal{M}_\chi$, thus incurring in truncation errors and breaking conservation laws. However, the TDVP-MPS aims to circumvent this limitations by locally optimizing the evolution within the manifold $\mathcal{M}_\chi$. It amounts to solve the Schrödinger

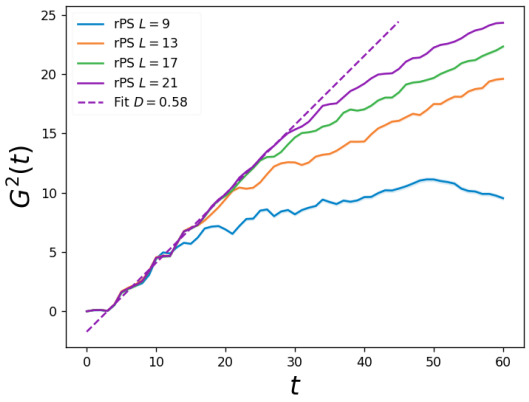

Figure 1. Measure of the diffusive spreading via the Gini coefficient for different L.

equation in the tangent space of $\mathcal{M}_\chi$:

$$\frac{d\,|\psi(t)\rangle}{dt} = -i\mathcal{P}_{\mathcal{M}_\chi} H\,|\psi(t)\rangle \quad (7)$$

where $\mathcal{P}_{\mathcal{M}_\chi}$ is the tangent space projector of $\mathcal{M}_\chi$. This method was shown to conserve all constant of motions such as expectation values of all generators of symmetries[32].

To measure the spreading of the local energy density after the quench,

$$E_j(t) = \left\langle \frac{J}{2} S_j^x S_{j+1}^x + \frac{J}{2} S_{j-1}^x S_j^x + h S_j^x + g S_j^z \right\rangle_{\rho(t)} \quad (8)$$

with $0 < j < L$, we consider the square of the Gini coefficient[33] which gives an alternative measure to the variance of the distribution:

$$G^2(t) = \left(2 \frac{\sum_i \sum_j E_i'(t) E_j'(t)\,|i-j|}{\sum_i \sum_j E_i'(t) E_j'(t)} \right)^2 \quad (9)$$

To guarantee that contributions to G^2 originate solely from the quench, we consider $E_j'(t) = E_j(t) - \overline{E(0^-)} - E_j(0)(1 - \delta_{j,L/2})$ where $\overline{E(0^-)}$ is the mean value of E_i over the chain before the quench. The advantage of G^2 when comparing to similar measures[34] is the robustness against random noise in the energy distribution. The diffusion coefficient, D, corresponds to a linear scaling $G^2(t) \propto Dt$, while ballistic transport scales as $G^2(t) \propto v_B^2 t^2$ with v_B the butterfly velocity.

III. Infinite temperature

We start by focusing on strong quenches, $\epsilon = 1$, at infinite temperature, $\beta = 0$. The spreading of the square of the Gini coefficient is depicted in Fig. (1) for consecutive larger chain sizes, $9 \leq L \leq 21$. We find three qualitatively different transport regimes. At very short

times, $t \lesssim t_1 = 3$, transport is anomalous, which can be attributed to initial development of entanglement between adjacent sites to the perturbation. This anomalous regime was already reported in Ref.[29] and will not play a role in our analysis. At intermediate times, and until a time $t^*(L)$ where the nature of the transport changes abruptly, we find a clear diffusive regime which is independent of the system size. We compute the diffusion constant via a linear fit for $L = 21$ and $t_1 < t < 29 = t^*(L = 21)$ obtaining $D = 0.58 \pm 0.01$. After the time $t^*(L)$, the transport is again anomalous with an overall diffusive nature for large chain sizes. We denote the abrupt change in transport that occurs at $t^*(L)$ as the breaking point and it bears all the similarities to a finite size effect. Surprisingly, this finite size effect is not related to the diffusive spreading, as it occurs before the diffusive component of the transport reaches the edge of the chain. An analysis of the breaking point as function of the system size reveals it scales linearly with a velocity $v^* = L/(2t^*) = 0.36 \pm 0.03$.

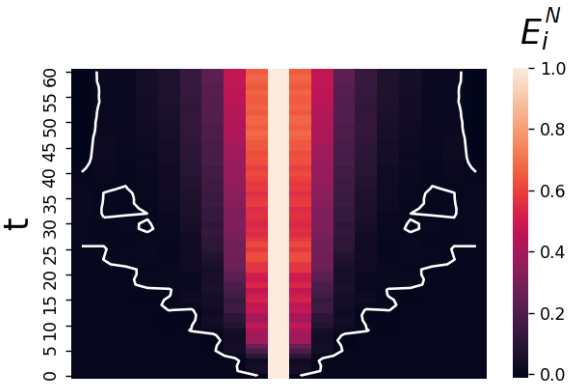

Figure 2. Normalized energy density plot with $L = 21$ and $\beta = 0$. Contour lines for $E_i^N = 0.003$ are depicted in white.

It is also worth analyzing the energy transport directly from the normalized energy density plot, $E_j^N = E_j(t)/\max_j(E_j(t))$, as shown in Fig. (2). The density plot is dominated by a diffusive bulk but a contour line for $E_i^N = 0.003$, depicted as white lines, reveals a ballistic wave front with a relative magnitude two orders of magnitude smaller than the diffusive core. This small ballistic component of the energy transport has the same velocity of the breaking point, v^*, motivating the idea that the breaking point signals the arrival of this ballistic component of the transport at the edge of the chain. It is unclear what the nature of this small ballistic component is, if it vanishes after some time or how it relates to other parameters of the simulation, such as temperature or quench's magnitude.

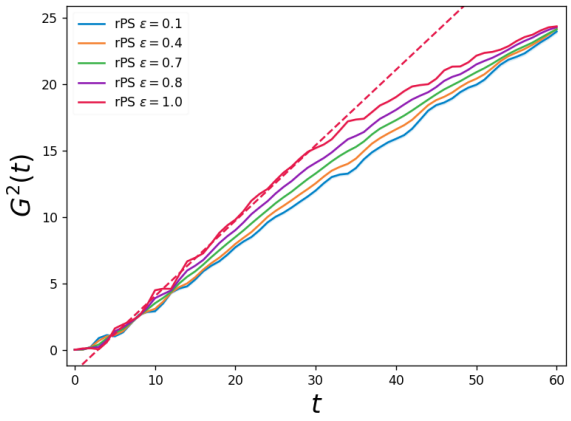

Figure 3. $G^2(t)$ for $L = 21$ as function of time for different quench parameters ϵ.

A. Magnitude of the quench

We study the energy transport for different magnitudes of the quench, ϵ, for a fixed system size of $L = 21$ at infinite temperature. In Fig. (3) we depict G^2 as function of t for consecutively small magnitudes. Qualitatively we find that the diffusion coefficient decreases for small ϵ and that the breaking point ceases to exist in the same limit. This seems to indicate that, in the limit $\epsilon \to 0$, G^2 converges to a straight line characteristic of a uniquely diffusive transport.

Note that the disappearance of the breaking point and the dependence of the diffusive constant with ϵ arise simultaneously. This suggests that, even though the small ballistic component of the energy transport does not affect the diffusive nature of the transport for $t_1 < t < t^*$, it does change the value of D.

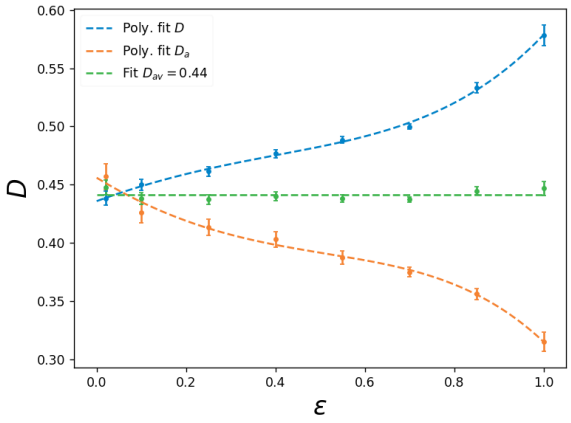

Figure 4. Dependence of the diffusion coefficient, D, with the magnitude of the quench, ϵ.

A quantitative analysis of the dependence of D with ϵ can be found in Fig. (4)-(blue dots), where we depict D obtained by a linear fit of G^2 for $3 < t < t^*$. The

scaling indicates that D converges to a finite value in the limit $\epsilon \to 0$; however, the dependence for finite ϵ is non-trivial. In Fig. (4)-(dashed blue line) we depict a third order polynomial fit.

The relation between the breaking point and the magnitude of the quench motivates us to study the energy transport for $t > t^*$. We assume that, close to t^*, the transport is also diffusive and extract a diffusion constant after t^*, D_a, fitting a straight line to $33 < t < 50$. This is depicted as orange dots in Fig. (4). Curiously, we find that the D_a is almost symmetric to D in the sense that the average diffusion, $D_{av} = (D_a + D)/2$, depicted as green dots, is almost independent of ϵ. Most importantly, D_{av} seems to coincide, within the error bar, with the predictions for $D(\epsilon \to 0)$. Further study near the vicinity of $\epsilon = 0$ is required to extract definite conclusions, but, if true, the diffusive component of the energy transport could still be obtained from a finite quench by taking into account the dynamics before and after the breaking point.

B. Product MPS

For the system sizes available with rPS, we cannot extract any information regarding a possible life-time of the small ballistic component beyond t^*. In particular, we are interested in knowing if the wave front propagates without dissipation or has some characteristic lifetime, after which energy only dissipates diffusively.

We use the ensemble of pMPS to probe the spreading in systems with $L = 41$ lattice sites and an estimated breaking point $t^*(L = 40) \approx 57$. In Fig. (5), we depict the average evolution of $N_s > 64 \times 10^3$ pMPS with bound dimension $\chi = 4, 8$ and compare it to the results from rPS for $L = 21$ (dashed black line and linear fit as blue line).

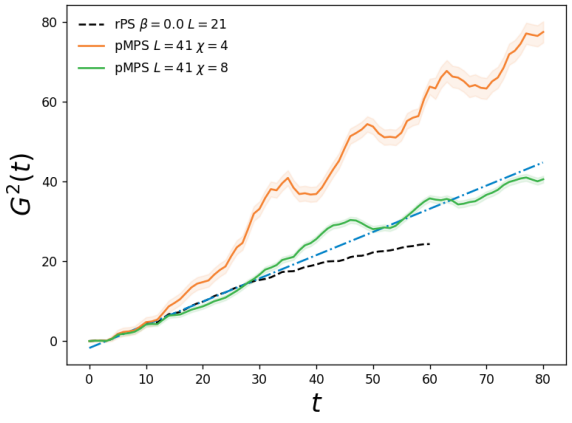

Figure 5. $G^2(t)$ for the ensemble of pMPS, for different bound dimensions.

We found that the ensemble of pMPS in conjugation with the TDVP-MPS fail to capture the correct dynamics even for small time scales $t \lesssim 20$ and presents strong anomalous behavior after that. In the next section, we present numerical evidence that this is not due to an anomalous transport for $L = 41$ but rather a flaw in the time evolution method itself in conjugation with G^2.

1. Edge-Bulk effect

In order to study the true origin of the deviations observed in Fig. (5), we question the validity of TDVP-MPS to time-evolve equilibrium ensembles, i.e. without any quench. By definition, an equilibrium ensemble commutes with the real time evolution propagator thus has no evolution or entanglement growth. However, the equilibrium ensemble is generated from many excited random states whose entanglement entropy grows in time and saturates eventually. In Fig. (6), we depict the time evolution of an equilibrium state at temperature $\beta = 1$ obtained averaging over $N_s = 10^5$ pMPS with bound dimension $\chi = 8$. Note that while deviations from the correct dynamics occur at all temperatures, the underlying cause is most prominent at finite temperature due to the anisotropy of the equilibrium state. Thus the choice of $\beta = 1$ and not $\beta = 0$.

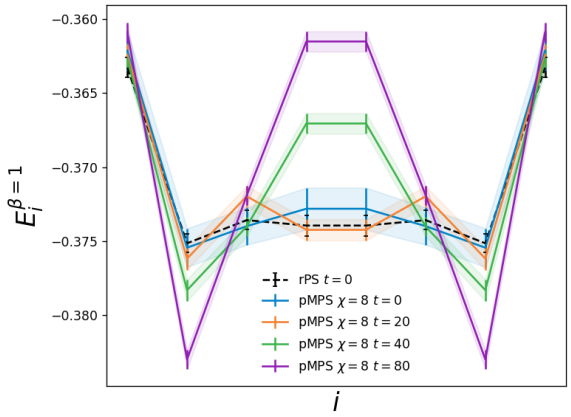

Figure 6. Time evolution of an unquenched thermal state at $\beta = 1$ for $\chi = 8$.

We observe that, within the error bar, the correct equilibrium ensemble is well captured at $t = 0$ and for small times, $t \lesssim 20$, the energy density profile remains constant. However, after $t = 20$ the local energy density of the bulk starts to increase while the energy density near the border decreases. We denote this effect by edge-bulk effect and it is a direct consequence of entanglement saturation in the chain. Once saturation occurs, the bound dimension at the bulk of the chain is no longer enough to locally describe the time evolved state, while near the edge the bound dimension is never saturated. This creates an unbalance: at each iteration, TDVP-MPS tries to minimize the local energy at the bulk while, due to energy conservation, any increase has to be counteracted by a decrease at the edge . The

final result is a deformed shape, as seen in Fig. (6). While the deformation is orders of magnitude smaller than the induced quench, it has important consequences in global measures of the spreading like G^2 as observed in Fig. (5).

Nevertheless it could still be possible to extract the correct diffusion coefficient from the thermalization of local observables near the center of the chain as was done in Ref.[27]. However, doing so, we discard important characteristics of the dynamics, such as the small ballistic component of the energy spreading.

IV. Finite temperature

It is important to understand how the multiple components of the dynamics found at $\beta = 0$, relate to the dynamics at finite temperatures. To our knowledge, this question has not been studied before in the context of the energy transport on the Ising chain. Physically, at high energies, a large number of degrees of freedom can be excited, therefore we expect a fast equilibration to the asymptotic long time regime. As temperatures decrease, a temperature-dependent equilibration time may emerge which delays the asymptotic long time regime. In this section, we study the energy transport in a strong quench at finite temperature. In a similar fashion to the previous section, we depict in Fig. (7) $G^2(t)$ for a fixed system size, $L = 21$, and different temperatures (full colored lines).

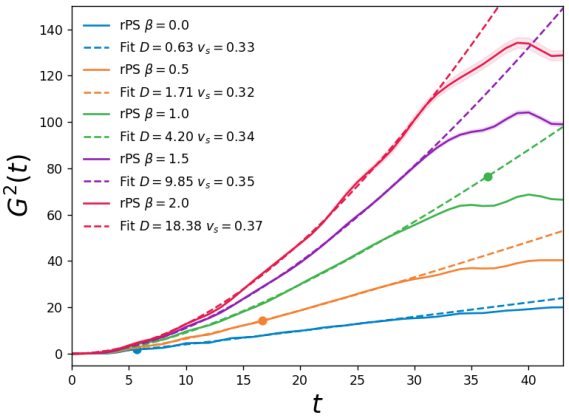

Figure 7. G^2 for different temperatures and $L = 21$ as function of time. Dashed lines depict a fitting of $1/\left((v_B t)^{-2} + (Dt)^{-1}\right)$.

Qualitatively we find that, as temperature decreases, ballistic transport becomes increasingly dominant at short time scales while diffusion takes place later in time and at a faster rate, i.e. it exists a temperature dependent crossover time scale between ballistic and diffusive transport, $\tau(\beta)$. To extract quantitative results, we model the spreading with an ansatz of the form $G^2(t) = 1/\left((v_B t)^{-2} + (Dt)^{-1}\right)$. This introduces a natural estimate for τ, namely that $\tau = D/v_B^2$. The ansatz is fitted for $t_1 < t < t^*$, with the best fit depicted in Fig. (7) as dashed colored lines and the crossover times, $\{\tau, G^2(\tau)\}$, as dots. The agreement with the data is surprisingly good, especially at intermediate temperatures where the transport in neither mostly ballistic or diffusive in the available time interval $t \in [3, t^*]$.

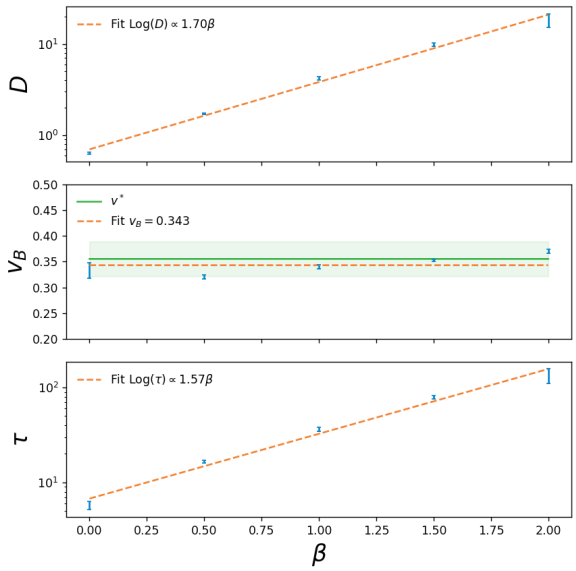

Figure 8. Fitting parameters of Fig. (7) as a function of β: diffusion constant, butterfly velocity and transition time scale, respectively upper, center and lower plots.

We plot the results from the fitting in Fig. (8): the diffusion constant, the butterfly velocity and the crossover time, respectively for upper, center an lower plot. The β dependence of the diffusion constant can be fitted to an exponential function, $D(\beta) = (0.70 \pm 0.07) \times \exp\left((1.70 \pm 0.08)\,\beta\right)$, for the available temperatures. It is not possible to study lower temperatures, $\beta > 2$, within the available system sizes because the crossover time is much larger than t^* and transport is almost purely ballistic for the times $t < t^*$. Most surprisingly, we find that the butterfly velocity is roughly independent of β,with a maximum variation of 8% with respect to the mean value, being compatible with $v_B(\beta) = 0.34 \pm 0.01$. We also compare $v_B(\beta)$ with the velocity of the breaking point v^* and show that both agree, within the error bar. This seems to suggest that the energy wave front at infinite temperatures and the ballistic transport at finite temperatures are one and the same, i.e. the wave front at high temperatures is a reminiscence of transport at low temperatures.

As a consequence of the previous considerations, the crossover scale τ must also growth exponentially for lower temperatures, in agreement with the qualitative observations that diffusive transport takes place latter in time for lower temperatures.

V. Discussion

In Ref.[29], the authors put forward a tempting hypothesis to explain the emergence of diffusive transport in non-integrable highly excited systems (infinite temperatures). They argue that, if a heuristic description of ballistic quasi-particle (QP) as carriers energy was possible (similar to integrable systems[35]), these QP would scatter strongly and often, i.e. short mean free path. At each collision, quantum information would be passed along in a ballistic wave front but the average path of a QP resembles a random walk. They conjecture that any local observables, under this conditions, would propagate diffusively.

We can extend this heuristic argument to finite temperatures. At infinite T, QP form often and randomly on the equilibrium ensemble; as T decreases, they do so less frequently an carry less energy (velocity). Therefore, the mean free path must increase and the previously restrained QP now propagate ballistically for longer times. This would be in line with results from Fig. (8), explaining both why τ increases and v_B remains constant. However, this heuristic picture does not explain the existence of a wave front of energy at $\beta = 0$ for $t > \tau$. We conjecture that for large quench parameters, the wave front is composed by high energy QP propagating at a maximum velocity. These, because they propagate outwards from the perturbation, contribute positively to G^2 but once they reflect on the edge the contribution changes sign leading to the breaking point observed in Fig. (7). As a side product of this argument we expect the contribution observed in Fig. (4) to vanish for very large times and system sizes. Note that this entire heuristic argument extends beyond our current numerical limits and should not be understood as a proof.

In conclusion, we found strong numerical evidence that at finite temperatures, transport in TLI model is ballistic until a time scale τ and becomes diffusive afterwards. This time scale depends exponentially on β for the temperatures studied here, but its dependence for very low temperatures is still unknown. Moreover, we found that the spreading at $\beta \neq 0$ could be well fitted to $G^2(t) = 1/\left((v_B t)^{-2} + (Dt)^{-1}\right)$ until a time t^* where a deviation occurs. This time, named breaking point, originates from a ballistic wave front of energy which exists at all temperatures and has the same velocity as the ballistic transport at finite temperatures. Curiously, the contribution of the wave front to G^2 depends quadratically with the strength of the quench, ϵ. We also found that the wave front contribution is symmetric immediately before and after the breaking point leading us to speculate whether reflection of some kind may occur at t^*. It would be interesting to derive analytic predictions for $D(\epsilon)$ and the affect of the breaking point by modeling the transport with a ballistic and diffusive component. Further understanding of the nature of the ballistic wave front requires a study of its long-time properties which, as we shown, could not be achieved with the combination of $G^2$and TDVP-MPS algorithm.

We believe it should be possible to incorporate these results in one common framework of transport in non-integrable models. A possible direction would be to develop further the heuristic picture and extract some quantitative predictions from it.

VI. Acknowledgments

The author thanks Professor F. Pollmann and Professor P. Ribeiro for the supervision of this work, T. Rakovszky for fruitful discussions as well as L. Silva and A. Costa for reviewing the manuscript. Part of this work has been supported by FCT through the Investigator FCT contract IF/00347/2014 and Grant No. UID/CTM/04540/2013.

[1] C. Gogolin and J. Eisert, Reports on Progress in Physics **79**, 056001 (2016), arXiv:1503.07538.
[2] L. E. Sadler, J. M. Higbie, S. R. Leslie, M. Vengalattore, and D. M. Stamper-Kurn, Nature **443**, 312 (2006), arXiv:0605351 [cond-mat].
[3] T. Kinoshita, T. Wenger, and D. S. Weiss, Nature **440**, 900 (2006).
[4] K. Kim, S. Korenblit, R. Islam, E. E. Edwards, M.-S. Chang, C. Noh, H. Carmichael, G.-D. Lin, L.-M. Duan, C. C. Joseph Wang, J. K. Freericks, and C. Monroe, New Journal of Physics **13**, 105003 (2011), arXiv:1107.0181.
[5] S. Sahling, G. Remenyi, C. Paulsen, P. Monceau, V. Saligrama, C. Marin, A. Revcolevschi, L. P. Regnault, S. Raymond, and J. E. Lorenzo, Nature Physics **11**, 255 (2015).
[6] S. Korenblit, D. Kafri, W. C. Campbell, R. Islam, E. E. Edwards, Z.-X. Gong, G.-D. Lin, L.-M. Duan, J. Kim, K. Kim, and C. Monroe, New Journal of Physics **14**, 095024 (2012), arXiv:1201.0776.
[7] M. Rigol, V. Dunjko, and M. Olshanii, Nature **452**, 854 (2008), arXiv:0708.1324.
[8] M. Sánchez and U. Granada, EAS Publications Series **30**, 201 (2008), arXiv:arXiv:0712.1933v2.
[9] M. Srednicki, Journal of Physics A: Mathematical and General **32**, 1163 (1999), arXiv:9809360 [cond-mat].
[10] F. Alet and N. Laflorencie, Comptes Rendus Physique (2018), 10.1016/j.crhy.2018.03.003, arXiv:arXiv:1711.03145v2.
[11] A. Nahum, J. Ruhman, and D. A. Huse, Physical Review B **98**, 035118 (2018), arXiv:1705.10364.
[12] E. Bairey, G. Refael, and N. H. Lindner, Physical Review B **96**, 020201 (2017), arXiv:1702.06208.
[13] P. Mazur, Physica **43**, 533 (1969).
[14] J. Sirker, R. G. Pereira, and I. Affleck, Physical Review Letters **103**, 216602 (2009), arXiv:arXiv:0906.1978v2.
[15] H. Bethe, Zeitschrift für Physik **71**, 205 (1931).

[16] V. E. Korepin, N. M. Bogoliubov, and A. G. Izergin, *Quantum Inverse Scattering Method and Correlation Functions* (Cambridge University Press, Cambridge, 1993).

[17] W. Fu and S. Sachdev, Physical Review B **94**, 035135 (2016), arXiv:1603.05246.

[18] V. Oganesyan and D. A. Huse, Physical Review B **75**, 155111 (2007), arXiv:0610854 [cond-mat].

[19] R. Orús and G. Vidal, Physical Review B **78**, 155117 (2008), arXiv:0711.3960.

[20] R. Steinigeweg, F. Heidrich-Meisner, J. Gemmer, K. Michielsen, and H. De Raedt, Physical Review B - Condensed Matter and Materials Physics **90**, 094417 (2014), arXiv:1406.2799.

[21] C. Karrasch, J. E. Moore, and F. Heidrich-Meisner, Physical Review B **89**, 075139 (2013), arXiv:1312.2938.

[22] J. Gemmer, M. Michel, and G. Mahler, in *Lecture Notes in Physics*, Vol. 784 (Springer Berlin Heidelberg, 2009) lect. note ed., pp. 77–83.

[23] C. Bartsch and J. Gemmer, Physical Review Letters **102**, 110403 (2009), arXiv:0902.0927.

[24] S. R. White, Physical Review Letters **102**, 190601 (2009), arXiv:arXiv:0902.4475v2.

[25] S. Garnerone, Physical Review B **88**, 165140 (2013), arXiv:1309.0851.

[26] S. Garnerone, T. R. de Oliveira, S. Haas, and P. Zanardi, Physical Review A **82**, 052312 (2010), arXiv:arXiv:1003.5253v2.

[27] E. Leviatan, F. Pollmann, J. H. Bardarson, D. A. Huse, and E. Altman, arXiv , 1 (2017), arXiv:1702.08894.

[28] J. Haegeman, C. Lubich, I. Oseledets, B. Vandereycken, and F. Verstraete, Physical Review B **94**, 165116 (2016), arXiv:1408.5056.

[29] H. Kim and D. A. Huse, Physical Review Letters **111**, 127205 (2013), arXiv:arXiv:1306.4306v1.

[30] J. S. Ferreira, (2018).

[31] J. Gemmer and G. Mahler, The European Physical Journal B - Condensed Matter **31**, 249 (2003), arXiv:0201136 [quant-ph].

[32] J. Haegeman, J. I. Cirac, T. J. Osborne, I. Pižorn, H. Verschelde, and F. Verstraete, Physical Review Letters **107**, 070601 (2011).

[33] C. Gini, Rivista di politica economica **87** (1997).

[34] B. Kloss, Y. B. Lev, and D. Reichman, (2017), 10.1103/PhysRevB.97.02430, arXiv:1710.09378.

[35] P. Calabrese and J. Cardy, Journal of Statistical Mechanics: Theory and Experiment **2005**, P04010 (2005), arXiv:0503393v1 [arXiv:cond-mat].